

Supplementary information

Nanoparticle-based highly sensitive MRI contrast agents with enhanced relaxivity in reductive milieu

Severin J. Sigg[†], Francesco Santini^{‡,§}, Adrian Najer[†], Pascal U. Richard[†], Wolfgang P. Meier[†],
and Cornelia G. Palivan^{†,*}

[†]Department of Chemistry, University of Basel, Klingelbergstrasse 80, 4056 Basel, Switzerland

[‡]Department of Radiology, Division of Radiological Physics, University of Basel Hospital, Petersgraben 4, 4031 Basel, Switzerland

[§]Department of Biomedical Engineering, University of Basel, Basel, Switzerland

MATERIALS AND METHODS

Materials. All reagents and materials were of the highest commercially available grade and were used without further purification, unless otherwise mentioned. 2-(6-chloro-1*H*-benzotriazole-1-yl)-1,1,3,3-tetramethyluronium hexafluoro-phosphate (HCTU), Rink Amide AM resin (0.71 mmol/g) and Fmoc-Trp(Boc)-OH were purchased from IRIS Biotech GmbH. Boc-Cystamine-Suc-OH was obtained from IRIS Biotech GmbH and converted to Fmoc-Cystamine-Suc-OH amino acid as previously described.¹ Other amino acids were ordered from Novabiochem. Dimethylformamide (DMF) was purchased from J.T. Baker, diisopropylethylamine (DIPEA) from VWR, dichloromethane (DCM) and ethanol (96 %) F15 from Brenntag Schweizerhall AG, and acetonitrile (ACN) from Fisher Scientific. Opti-MEM, DMEM, fetal bovine serum, and penn/strep were obtained from Gibco. CellTiter 96 Aqueous One Solution Cell Proliferation Assay (MTS) was purchased from Promega. Heparin sodium salt from porcine intestinal mucosa (15 kDa, 193 U/mg) was purchased from Merck KGaA (Darmstadt, Germany), Aminopropyl-terminated poly(dimethylsiloxane) (PDMS(NH₂)₂) was obtained from ABCR GmbH (Karlsruhe, Germany). All other chemicals and reagents were

ordered from Sigma-Aldrich. Free amines in DMF were eliminated by aluminum oxide prior to usage. Dialysis was performed in dialysis tubings from Spectrum Laboratories (Spectrum Laboratories Inc., cellulose ester, MWCO 0.5–1 kDa or 3.5–5 kDa). Water was obtained from a Milli-Q Direct 8 water purification system (Merck Millipore).

Heparin-PDMS synthesis. Heparin-PDMS block copolymer was synthesized as reported previously.² Briefly, heparin sodium salt was converted to tetrabutylammonium salt using a Dowex Marathon MSC column (Sigma-Aldrich, 428787) neutralizing to pH 7 with tetrabutylammonium hydroxide solution (Sigma-Aldrich, 86863). The product was purified via dialysis against water for at least 48 h (Spectrum Laboratories Inc., CA, USA, MWCO 3.5–5 kDa) and dried. Heparin tetrabutylammonium salt was reacted with PDMS(NH₂)₂ for 7 days, then precipitated in diethyl ether, washed, purified and dried.

Peptide synthesis. Peptides were synthesized as described previously.³ Briefly, peptides were synthesized by solid phase peptide synthesis using a Syro I peptide synthesizer (MultiSyn Tech GmbH, Witten, Germany) using standard fluorenylmethoxycarbonyl (Fmoc) chemistry and HCTU coupling protocols. After synthesis, the resin was isolated and washed alternating with DMF, methanol, and dichloromethane. Cleavage from the resin and removal of protective groups was performed for 2 h in 10 mL cleavage cocktail containing 85% trifluoroacetic acid (TFA), 2.5% triisopropylsilane, 2.5% ethanedithiol, 5% thioanisole and 5% H₂O followed by filtration and precipitation in 40 mL cold diethyl ether. The pellet was subsequently solubilized and lyophilized. Purification was performed on a high-performance liquid chromatography (HPLC) instrument from Shimadzu using a C18 reverse phase (RP) column (Merck Chromolith, RP-18e, 100 mm × 10 mm and 100 mm × 4.6 mm) with mobile phases of water and acetonitrile containing 0.1% TFA while monitoring at 280 nm. Correct mass was confirmed by liquid chromatography electron spray ionization mass spectrometry (LC-ESI-MS) performed on an amazon X MS from Bruker (Germany).

Gadolinium-complex and nanoparticle formation and characterization. HepPDMS was dissolved in 50% ethanol and filtered (0.45 μm) to obtain a 17 mg/mL clear solution. After dilution to 4.25 mg/mL and pH adjustment to pH 7 using diluted NaOH, the solution was dialyzed against water for 16 h, renewing exchange solvent twice, using prewashed 0.5-1 kDa MWCO dialysis tubes. HepPDMS-Gd nanoparticles were formed by adding gadolinium chloride hexahydrate stock solution (27 mM) dropwise under stirring to above described hepPDMS stock solution (17 mg/mL). The pH was readjusted to 7 when necessary, diluted to 4.25 mg/mL HepPDMS and to a final gadolinium concentration of 2.4 mM, then dialyzed to water as described above. For production of coassemblies the peptides were first dissolved in 50% ethanol to obtain 1 mg/mL stock solutions and then filtered through 0.2 μm hydrophilic syringe filters. HepPDMS-Gd stock solutions (8.5 mg/mL) were mixed 1:1 with peptide stock solution and subsequently dialyzed as described above. After sample removal from dialysis tubing, the hydrodynamic diameter was measured from diluted samples in water (1:10 v:v) by dynamic light scattering (DLS), zeta-potential was measured at 1:100 (v/v) dilution in water. DLS and zeta-potential data were obtained from a Zeta Sizer Nano ZSP (Malvern Instruments Ltd., UK) operating at a fixed angle of $\theta = 173^\circ$ with a laser beam wavelength of 633 nm at room temperature. Transmission electron microscope (TEM) images were recorded using a Philips CM100 transmission electron microscope operating at an acceleration voltage of 80 kV. Samples were incubated for 2 min on hydrophilized, carbon coated, parlodion-(2% in n-butyl acetate) copper grids, when necessary the grids were negatively stained for 10 s with a 2% uranyl acetate solution. Size data was obtained using the imageJ64 program ($n > 100$). For energy dispersive X-ray spectroscopy (EDX) analysis an FEI Nova NanoSEM was used operating at 10 kV. Samples were prepared on glass coverslips and sputter-coated with silver.

Cell culture. HeLa cells were maintained at 37 °C in a 5% CO₂ and were grown in Dulbecco's modified eagle medium (DMEM) with 10% fetal bovine serum (FBS), 100 units/mL penicillin and 100 µg/mL streptomycin.

Cell viability assay. Cytotoxicity testing was performed using the Promega CellTiter 96 AQueous Non-Radioactive Cell Proliferation (MTS) assay determining the number of viable cells in culture. 2×10^3 HeLa cells were seeded in triplicates in a 96-well plate 24 h prior to the experiment. 10 µL of peptide HepPDMS-Gd NPs were added to the cells to give final concentrations between 0.05–1 mM Gd and incubated for 24 h at 37°C with 5% CO₂. MTS solution (20 µL/well) was added to the cells and incubated for 2 h. Cell viability was calculated by measuring the absorbance at 490 nm using a SpectraMax M5^e (Molecular Device) spectrometer, and data was normalized where minimum viability was media and MTS assay alone and maximum viability was cells incubated with 10 µL equivalents of water.

Cellular uptake. HeLa cells (5×10^4 cells per well) were seeded in triplicates into a 24-well chamber 24 h prior to the experiment. The cell culture media was replaced with Opti-MEM (150 µL) followed by addition of 20 µL peptide HepPDMS-Gd nanoparticles. After 4 h incubation, the cell culture medium was removed and replaced with serum-containing medium (500 µL). The cells were then incubated for another 20 h. Cells were washed with opti-MEM, trypsinized, transferred to Falcon tubes and digested in 65% HNO₃ over night. Subsequently, the gadolinium-content was determined using inductively coupled plasma optical emission spectroscopy (ICP-OES).

ICP-OES. All gadolinium contents were determined by ICP-OES. Quantification of gadolinium was carried out on a Ciros Vision inductively coupled plasma optical emission spectroscopy from Spektro (Kleve, Germany) in axial mode. Gadolinium stock solutions of known metal content were measured prior to sample measurements to plot calibration curves. All samples were digested by 65% HNO₃ overnight and diluted to 2% HNO₃ prior to analysis.

Anticoagulation activity. The anticoagulation activity was determined by a Biophen Heparin (LRT) kit using a STA-R analyzer from Stago and the absorbance was measured at 405 nm.

Farndale microassay. Accessible heparin was determined by Farndale microassay as described previously.^{2,4} Briefly, 250 μ l 1,9-dimethylmethylene blue (DMMB) stock solution was mixed with 50 μ l heparin standards (2.5–20 μ g/mL). Samples were diluted to the range of the calibration curve using phosphate buffered saline (PBS). Absorption was measured at 525 nm and the heparin levels of samples were calculated using a standard dilution curve.

Xylenol orange assay. Free gadolinium levels were analyzed by xylenol orange assay according to a published procedure.⁵ Briefly, xylenol orange tetrasodium salt was diluted in 10 mM HEPES buffer pH 6 to obtain a 12 μ g/mL stock solution. Samples were diluted to the linear range and 10 μ L aliquots were mixed with 100 μ L xylenol orange stock solution. For stability tests samples were maintained in optiMEM with FBS, after 7 days 10 μ L sample was added to 100 μ L stock solution in triplicates and measured absorption at 433 nm and 473 nm. Gadolinium-ion concentration was calculated using a calibration curve of the ratio of absorption at 573 nm and 433 nm plotted against gadolinium-concentration.

Electron Paramagnetic Resonance Spectroscopy. Electron paramagnetic resonance (EPR) spectra were recorded with a Bruker ElexSys500 X-band CW spectrometer, to which the superQ wave-guide resonance cavity (ER4122 SHQE-W1) was attached. Microwave power was adjusted at levels below the saturation condition with values 2.0–6.0 mW. The modulation frequency was 100 kHz and the modulation amplitude was 0.9 mT; other spectral parameters were adjusted for each spectrum individually. 80 spectra were acquired to optimize the signal-to-noise ratio, and 3rd-order polynomial averaging was used for subsequent noise reduction. Gd samples (pH adjusted to 7 with NaOH) were measured at room temperature. Lorentzian line shapes were considered with the line-width adjusted for each spectrum. The peak-to-peak line width (ΔH_{pp}) was measured from the spectrum using

the WINEPR software. The transverse electronic relaxation rates, $1/T_{2e}$ were calculated using eq.1:⁶

$$\frac{1}{T_{2e}} = \frac{g\mu_B\pi\sqrt{3}}{h} \Delta H_{pp} \quad (1)$$

Where μ_B is the Bohr magneton, and h the Plank constant.

Magnetic resonance imaging (MRI). Samples were measured in 1.5 mL centrifuge vials in denoted concentrations. For imaging a 3T clinical human MRI scanner (Magnetom Prisma, Siemens Healthcare, Erlangen, Germany) was used. The T_1 relaxation times were measured using an inversion-recovery-prepared spin echo sequence with the following acquisition parameters: voxel size $1.2 \times 1.2 \times 5 \text{ mm}^3$, TR/TE 6000/12 ms. The scan was repeated at various inversion times (TI): 50 ms, 100 ms, 200 ms, 500 ms, 750 ms, 1000 ms, and 2000 ms. The T_2 relaxation times of the samples were measured using a multi-echo spin echo sequence with the following acquisition parameters: voxel size $1.2 \times 1.2 \times 5 \text{ mm}^3$, TR 3000 ms. 32 echoes were acquired with a 13.2 ms echo spacing (first echo: 13.2 ms, last echo: 422.4 ms).

Supplementary figures and tables

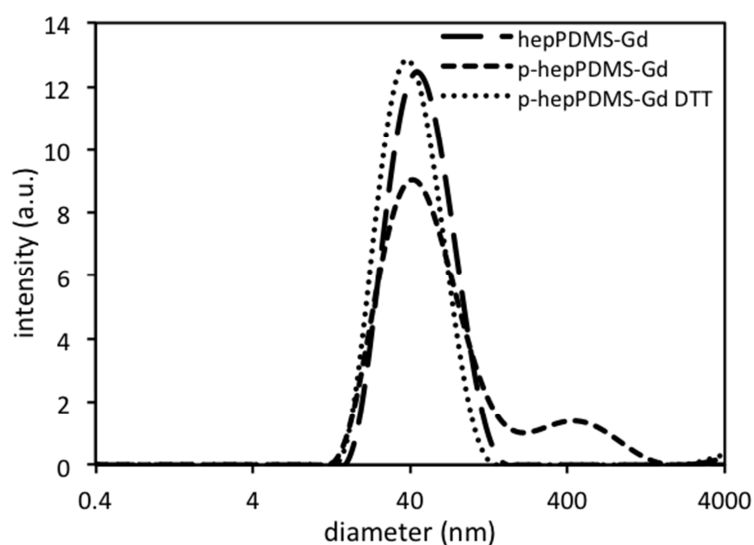


Figure S1. DLS of hepPDMS-Gd-NPs, p-hepPDMS-Gd-NPs (-DTT), and p-hepPDMS-Gd-NPs (+DTT).

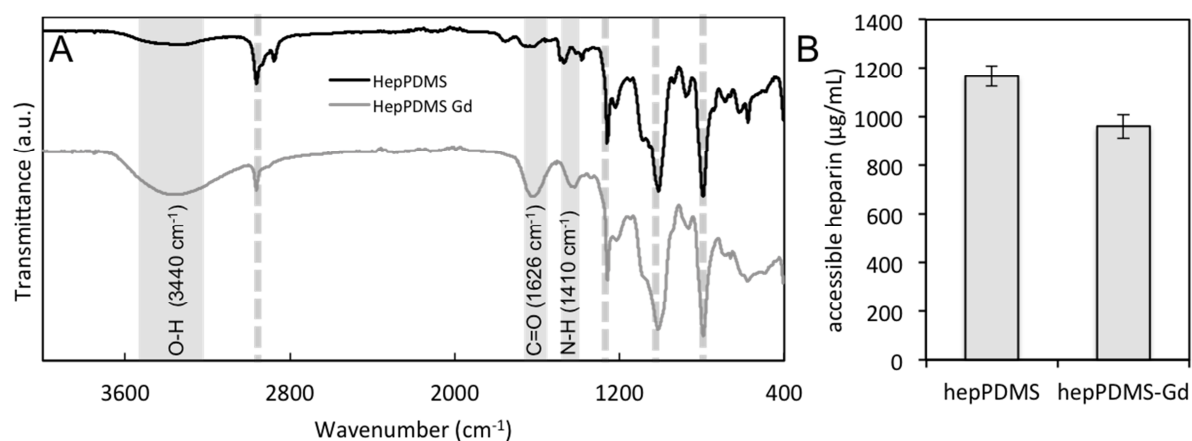


Figure S2. (A) FTIR spectra of hepPDMS-NPs and hepPDMS-Gd-NPs. Grey dashed lines are the PDMS absorptions that remain unchanged in presence of Gd, excluding interaction between PDMS and Gd; grey regions indicate the gadolinium interaction to the heparin block. (B) Surface accessible heparin as measured by Farndale microassay. Data represent average \pm SD ($n=3$).

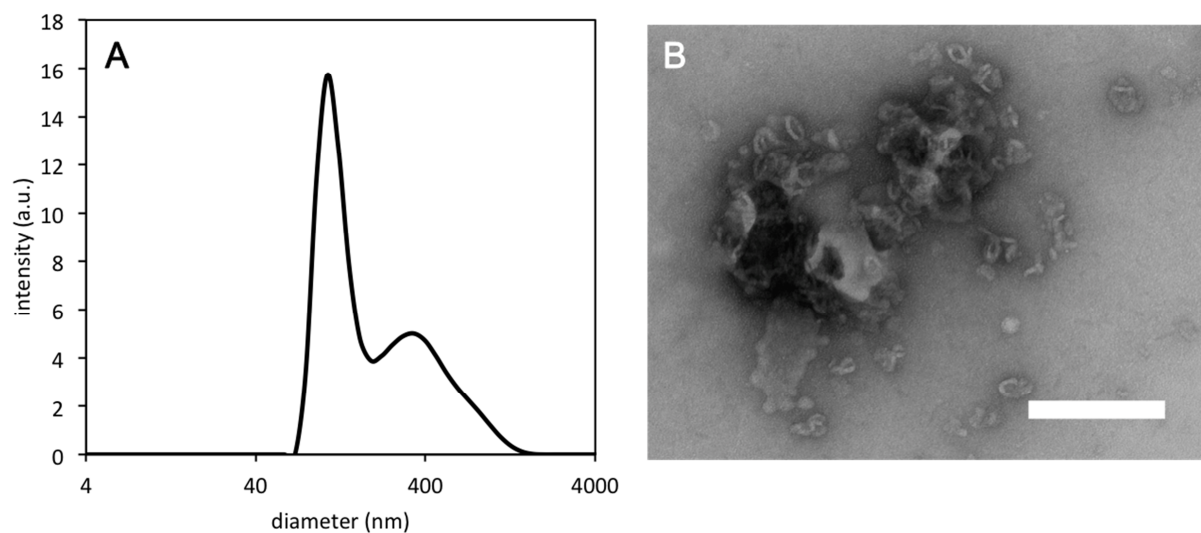


Figure S3. (A) DLS and TEM (B) of coassemblies formed using 2 mg/mL H3SSgT peptide, scale bar: 200 nm. At this concentration of peptide, larger size aggregates are formed along with the co-assemblies, thus a concentration of 0.5 mg/ml was used for all other characterization.

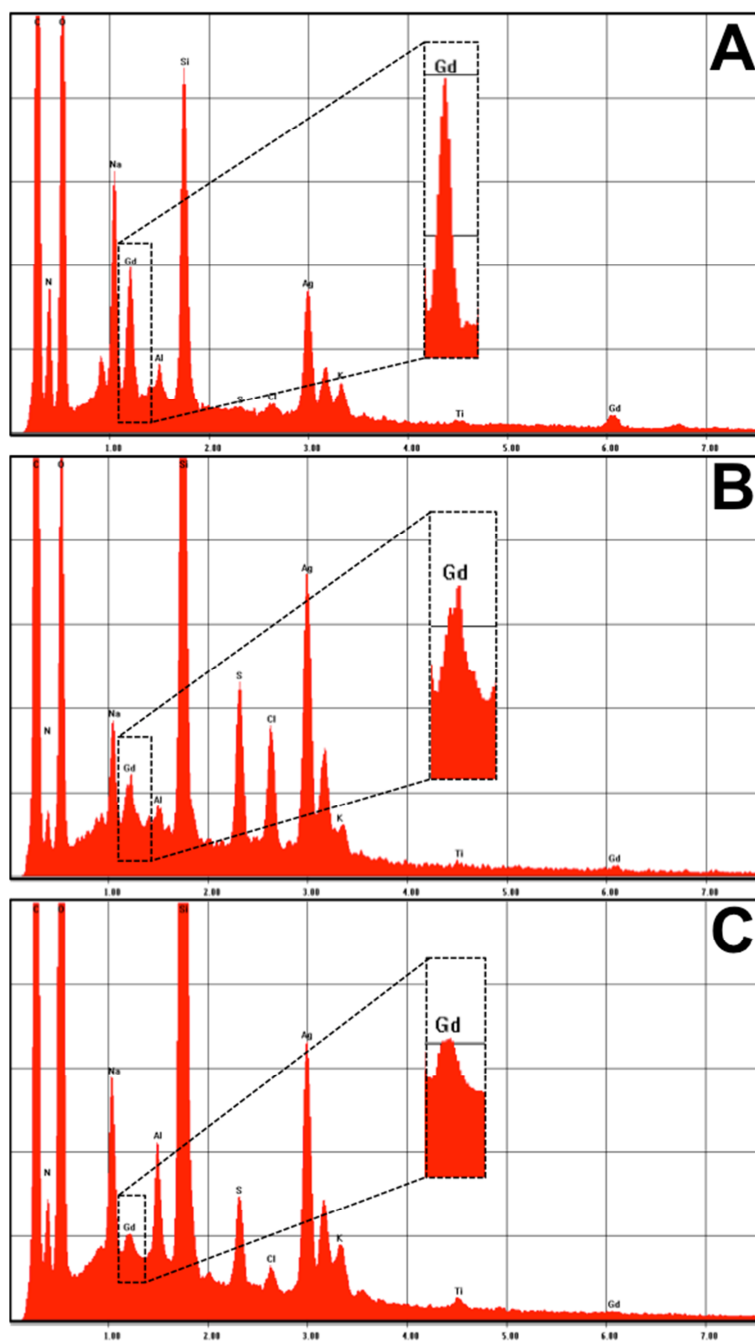


Figure S4. EDX-spectra of Gd-DOTA (A), hepPDMS-Gd NPs (B), and p-hepPDMS-Gd-NPs (C).

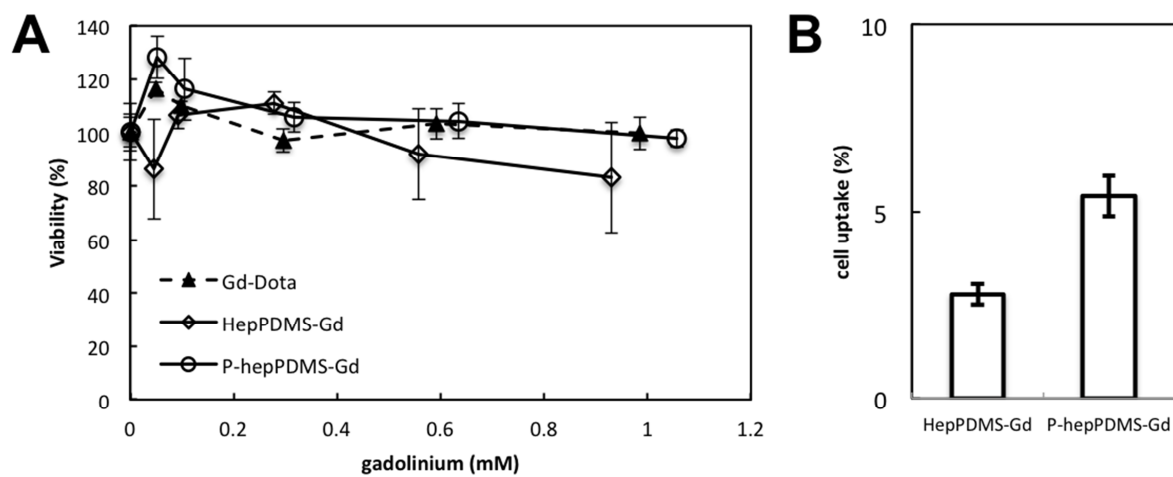


Figure S5. MTS viability assay of HepPDMS-Gd-NPs and p-hepPDMS-Gd-NPs compared to commercial contrast agent Gd-DOTA (A). Cell uptake of hepPDMS-Gd-NPs and p-HepPDMS-Gd-NPs (B). Data represent average \pm SD (n=3) (A); average \pm 10% deviation by ICP-OES (B).

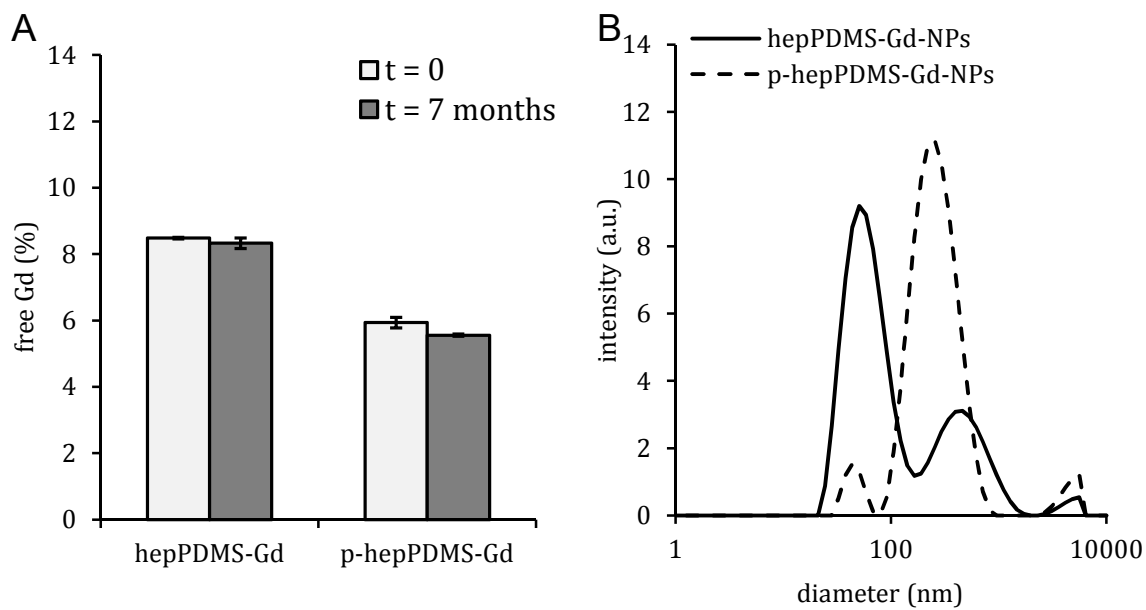


Figure S6. Free Gadolinium before and after incubation for 7 months at room temperature (A). Size distribution after incubation for 7 months (B).

Table S1. Longitudinal (T_1) and transverse (T_2) water protons relaxation times at various CA concentrations.

	Gd-concentration (mM)	T_1 (ms)	T_2 (ms)	r_1 ($\text{mM}^{-1}\text{s}^{-1}$)	r_2 ($\text{mM}^{-1}\text{s}^{-1}$)
Gd-DOTA	0.986	213	204	4.5 ± 0.1	4.90 ± 0.03
	0.591	334	341		
	0.296	632	680		
	0.099	1360	1870		
hepPDMS-Gd-NPs	0.930	20.2	6.79	51.7 ± 1.2	162.6 ± 17.8
	0.558	31.9	14.9		
	0.279	59.8	30.5		
	0.093	164	94.9		
p-hepPDMS-Gd-NPs (-DTT)	1.057	20.5	9.18	44.2 ± 1.5	103.5 ± 5.0
	0.634	31.6	17.0		
	0.317	57.9	33.6		
	0.106	154	98.5		
p-hepPDMS-Gd-NPs (+DTT)	1.057	16.7	8.73	54.4 ± 1.5	108.4 ± 2.5
	0.634	25.9	15.2		
	0.317	48.6	30.7		
	0.106	124	86.8		

Table S2. EPR parameters and transverse electronic relaxation times for Gd-DOTA and the Gd-NPs.

	g	ΔH_{pp} [G]	T_{2e} [ns]
Gd-DOTA	1.980	96	0.77
hepPDMS-Gd-NPs	2.003	430	0.15
p-hepPDMS-Gd-NPs	2.013	390	0.17

Comparison of r_1 relaxivities with literature

In literature, the relaxivity of experimental contrast agents (CAs) is determined at different magnetic fields, depending on the purpose of the study and/or the equipment available to the researcher. As the relaxivity is field dependent, the comparison between studies is rendered difficult, and we, herein, restrict ourselves to comparison with systems characterized in similar conditions.

At a magnetic field of 3 Tesla (corresponding to a proton Larmor frequency of 128MHz), the per Gd ion r_1 relaxivity of our system is in the range of 44-51 $\text{mM}^{-1}\text{s}^{-1}$. At the same magnetic field, clinically applied Gd-based CAs have r_1 relaxivities ranging from 2.8 $\text{mM}^{-1}\text{s}^{-1}$ for Prohance® to 4.0 $\text{mM}^{-1}\text{s}^{-1}$ for Multihance®.⁷

Lowering the tumbling rate of Gd-complexes through for example the formation of bulky assemblies is known to increase the relaxivity of the system. Examples of macromolecular Gd complexes and assemblies investigated at 3T include the experimental Gadomer 17, a polylysine dendrimer with 24 Gd-DOTA complexes having an r_1 relaxivity of 13.0 $\text{mM}^{-1}\text{s}^{-1}$.⁷ Other examples include Gd-polydisulfide copolymers (6.8 $\text{mM}^{-1}\text{s}^{-1}$)⁸, Gd-chelate functionalized copper sulfide NPs (8.65 $\text{mM}^{-1}\text{s}^{-1}$)⁹, colloidal structures obtained from miniemulsion polymerization of Gd-based metallosurfactants (11.1 $\text{mM}^{-1}\text{s}^{-1}$)¹⁰, various silica NPs entrapping or functionalized with Gd complexes (7.8-39.3 $\text{mM}^{-1}\text{s}^{-1}$)¹¹, copolymers containing Gd chelates (4.5-12.6 $\text{mM}^{-1}\text{s}^{-1}$)¹², and other dendrimers conjugated to Gd complexes (12-29 $\text{mM}^{-1}\text{s}^{-1}$).¹²

Although some systems with similar or higher relaxivities have been reported¹¹⁻¹³, to the best of our knowledge they were all measured at lower magnetic fields thus preventing direct comparison. Indeed, the relaxivity depends on the magnetic field in a nonlinear manner as illustrated by the covalent attachment of Gd chelates to thiolated DNA decorating gold nanoparticles or nanostars, where relaxivities of 14.6 and 54.7 $\text{mM}^{-1}\text{s}^{-1}$ measured at 1.41T (60MHz) drop significantly to, respectively, 5.8 and 9.4 $\text{mM}^{-1}\text{s}^{-1}$ at 7T (300MHz).¹³

Figure 2 discussion :

A T_1 weighted MR image, recorded on a human clinical 3T MRI scanner, of a) Gd-DOTA, b) hepPDMS-Gd-NPs, c) p-hepPDMS-Gd-NPs (-DTT), and d) p-hepPDMS-Gd-NPs (+DTT) with the concentration of each sample, given in white (values available in table S1). A decrease in longitudinal relaxation time (T_1) of water protons is observable with increase of Gd^{3+} concentration for each sample. Comparison of a) and b) indicates a much shorter relaxation time for the solution containing hepPDMS-Gd-NPs than for the solution containing Gd-DOTA at similar concentrations. The peptide containing nanoparticles (c) also exhibit a much smaller T_1 compared to Gd-DOTA. The measured T_1 is very similar for the particles with and without peptide, yet the concentration of the latter is smaller. Comparison of c) and d) shows a clear decrease in T_1 in presence of DTT, which is in agreement with the cleavage of the reduction sensitive bond in the peptide.

B EPR spectra of a) Gd-DOTA, b) hepPDMS-Gd-NPs, c) p-hepPDMS-Gd-NPs (-DTT) recorded at room temperature. The characteristic g-factors (table S2) are all around 2.00 within experimental error, with no additional lines at higher or lower g-values. Compared to Gd-DOTA (a), the spectra of Gd-containing NPs have very broad lines, resulting in significantly different transverse electronic relaxation times, T_{2e} (table S2). The significant difference between the transverse electron spin relaxation time corresponding to Gd-DOTA and those of Gd-NPs can be explained by intramolecular dipole-dipole interactions between close Gd^{III} ions within one NP, a distribution of multiple paramagnetic sites with different geometries within the particle and a slower rotational correlation time due to the difference in their size. Our results are in agreement with previous reports indicating that the increased proton relaxivity was associated with the formation of rigid micelle-like structures in aqueous solution.⁶ The slight difference in the transverse electron spin relaxation rate between Hep-PDMS-NP and Hep-PDMS-pept-NP indicate an effect of the peptide coating, as it has been intended in order to prevent Gd^{III} accessibility in other conditions than inside cells.

C Plot of the longitudinal relaxation rate ($1/T_1$) as a function of Gd^{3+} concentration for p-hepPDMS-Gd (+DTT) (squares), p-hepPDMS-Gd (-DTT) (circles), and Gd-DOTA (triangles) (values in table S1). The slope of the obtained curves is the relaxivity r_1 . Gd-DOTA (triangles) has a low relaxivity of $4.5 \pm 0.1 \text{ mM}^{-1} \text{ s}^{-1}$. For p-hepPDMS-Gd-NPs (circles), the longitudinal relaxivity is $44.2 \pm 1.5 \text{ mM}^{-1} \text{ s}^{-1}$ and increases to $54.4 \pm 1.5 \text{ mM}^{-1} \text{ s}^{-1}$ upon treatment with DTT (squares), resulting in a relaxivity more than an order of magnitude higher than Gd-DOTA.

D Same than **C** for the transverse relaxation rate ($1/T_2$). The trend is similar to the one observed for T_1 .

REFERENCES

1. F. Thielbeer, S. V. Chankeshwara, E. M. V. Johansson, N. Norouzi and M. Bradley, *Chem. Sci.*, 2013, **4**, 425-431.
2. A. Najer, D. Wu, A. Bieri, F. Brand, C. G. Palivan, H.-P. Beck and W. Meier, *ACS Nano*, 2014, **8**, 12560-12571.
3. S. J. Sigg, V. Postupalenko, J. T. Duskey, C. G. Palivan and W. Meier, *Biomacromolecules*, 2016, **17**, 935-945.
4. I. Barbosa, S. Garcia, V. Barbier-Chassefière, J.-P. Caruelle, I. Martelly and D. Papy-Garcia, *Glycobiology*, 2003, **13**, 647-653.
5. A. Barge, G. Cravotto, E. Gianolio and F. Fedeli, *Contrast Media Mol. Imaging*, 2006, **1**, 184-188.
6. G. M. Nicolle, É. Tóth, H. Schmitt-Willich, B. Radüchel and A. E. Merbach, *Chem. - Eur. J.*, 2002, **8**, 1040-1048.
7. M. Rohrer, H. Bauer, J. Mintorovitch, M. Requardt and H. J. Weinmann, *Invest Radiol*, 2005, **40**, 715-724.
8. C. H. Huang and A. Tsourkas, *Curr Top Med Chem*, 2013, **13**, 411-421.
9. S. Zhang, Z. Zha, X. Yue, X. Liang and Z. Dai, *Chem Commun (Camb)*, 2013, **49**, 6776-6778.
10. P. Gong, Z. Chen, Y. Chen, W. Wang, X. Wang and A. Hu, *Chem Commun (Camb)*, 2011, **47**, 4240-4242.
11. M. A. Bruckman, X. Yu and N. F. Steinmetz, *Nanotechnology*, 2013, **24**, 462001.
12. J. Tang, Y. Sheng, H. Hu and Y. Shen, *Prog. Polym. Sci.*, 2013, **38**, 462-502.
13. M. W. Rotz, K. S. Culver, G. Parigi, K. W. MacRenaris, C. Luchinat, T. W. Odom and T. J. Meade, *ACS Nano*, 2015, **9**, 3385-3396.